

The de novo centriole assembly pathway in HeLa cells: cell cycle progression and centriole assembly/maturation

Sabrina La Terra,^{1,2} Christopher N. English,³ Polla Hergert,¹ Bruce F. McEwen,^{1,2} Greenfield Sluder,³ and Alexey Khodjakov^{1,2}

¹Wadsworth Center, New York State Department of Health, Albany, NY 12201

²Department of Biomedical Sciences, State University of New York, Albany, NY 12222

³Department of Cell Biology, University of Massachusetts Medical School, Worcester, MA 01605

It has been reported that nontransformed mammalian cells become arrested during G₁ in the absence of centrioles (Hinchcliffe, E., F. Miller, M. Cham, A. Khodjakov, and G. Sluder. 2001. *Science*. 291:1547–1550). Here, we show that removal of resident centrioles (by laser ablation or needle microsurgery) does not impede cell cycle progression in HeLa cells. HeLa cells born without centrosomes, later, assemble a variable number of centrioles de novo. Centriole assembly begins with the formation of small centrin aggregates that appear during the S phase. These, initially amorphous “precentrioles”

become morphologically recognizable centrioles before mitosis. De novo–assembled centrioles mature (i.e., gain abilities to organize microtubules and replicate) in the next cell cycle. This maturation is not simply a time-dependent phenomenon, because de novo–formed centrioles do not mature if they are assembled in S phase–arrested cells. By selectively ablating only one centriole at a time, we find that the presence of a single centriole inhibits the assembly of additional centrioles, indicating that centrioles have an activity that suppresses the de novo pathway.

Introduction

The centrosome in somatic cells consists of two centrioles surrounded by a cloud of amorphous pericentriolar material (PCM) containing the γ -tubulin ring complexes involved in microtubule nucleation (Moritz et al., 1995; Zheng et al., 1995; Schnackenberg et al., 1998). Because the PCM accumulates around the centrioles (Bobinnec et al., 1998), the number of centrioles ultimately defines the number of functionally active centrosomes in the cell (Rieder et al., 2001).

New or “daughter” centrioles normally form in association with preexisting “mother” centrioles approximately at the G₁/S transition. The mother and the daughter remain physically linked until after the ensuing mitosis (Vorobjev and Chentsov, 1982; Rieder and Borisy, 1982). As a result, each daughter cell inherits one centriole that is <1 cell cycle old and one that was formed ≥ 1.5 cell cycles ago. The assembly of just a single new centriole in close spatial association with the mother indicates that centriole formation normally requires a special site for its assembly, which is present only in the proximal end of a mature

centriole. This ensures that centriole duplication is under tight numerical and spatial control. Failure of the cell to precisely regulate centrosome number leads to multipolar mitotic spindles and unequal chromosome distribution at mitosis. This, in turn, results in aneuploidy, genetic imbalances, and genomic instability that are hallmarks of aggressive human tumors (for reviews see Brinkley, 2001; Salisbury et al., 1999).

Under certain circumstances, centrioles can also assemble de novo. This process has been reported in a number of cell types, including lower eukaryotes (Marshall et al., 2001; Suh et al., 2002), oocytes (Palazzo et al., 1992), blastomers (Szollosi et al., 1972), and parthenogenetically developing embryos (Kallenbach and Mazia, 1982; Szollosi and Ozil, 1991; Riparbelli and Callaini, 2003). The de novo assembly has also been observed in vertebrate somatic cells, albeit only in CHO cells artificially arrested in S phase (Khodjakov et al., 2002). In this system, the de novo pathway results in simultaneous formation of a variable number of centrosomes over 24 h, which is the time comparable with the duration of the cell cycle in these cells.

The practical significance of the de novo pathway remained unclear, because normal vertebrate somatic cells, from which the centrosome has been removed, arrest in G₁ and do not form centrosomes de novo (Maniotis and Schliwa, 1991; Hinchcliffe

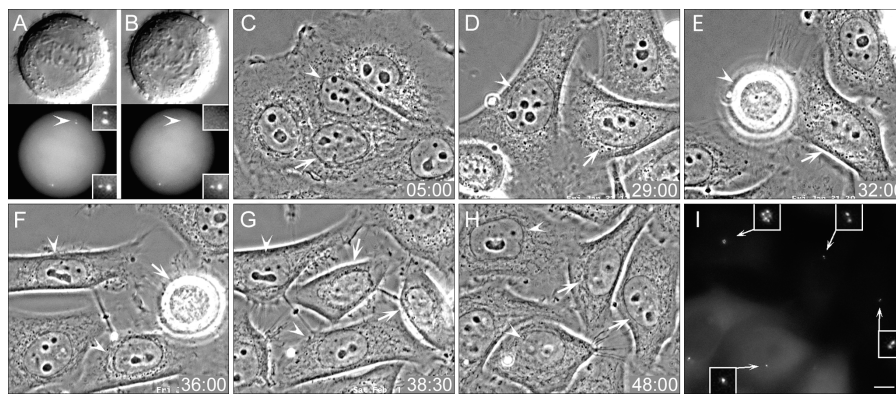
Correspondence to Alexey Khodjakov: khodj@wadsworth.org

Abbreviations used in this paper: 3-D, three-dimensional; PCM, pericentriolar material.

The online version of this paper contains supplemental material.

Figure 1. HeLa cells born without centrosomes continue to progress through the cell cycle.

(A and B) DIC (top) and fluorescence images (bottom) of a metaphase cell before (A) and after (B) laser ablation of one of the two centrosomes (A and B, compare arrowheads). Insets show centrioles at a higher magnification. (C–H) Selected phase-contrast frames from the multimode time lapse video recording of this cell. Arrowheads mark the cell born without centrosome, and arrows point at its sister that inherited the normal centrosome. Both cells undergo normal postmitotic flattening (C) and are morphologically similar to each other and non-irradiated cells (D). The cell born without a centrosome undergoes mitosis 32 h after the operation (E), and its sister follows just 4 h later (F). (I) GFP fluorescence (maximal-intensity projection) reveals that 48 h after the operation, one progeny of the cell born without a centrosome contains one centrin/GFP aggregate, whereas its sister contains seven centrin/GFP aggregates. Each of the two progeny of the sister cell that inherited a normal centrosome contains two centrin/GFP aggregate (centrioles). Insets show centrin/GFP aggregate at a higher magnification. Time is shown in hours:minutes. Bar, 5 μ m.



et al., 2001; Khodjakov and Rieder, 2001). Thus, to further advance our understanding of de novo centrosome formation in mammalian cells, we sought to test if this phenomenon is peculiar to CHO cells arrested in S phase. We turned to HeLa cells because their cell cycle may be less stringently linked to the presence of the centrosome than it is in other cell types. HeLa cells can progress through the cell cycle when the centrosome is dispersed by microinjection of antipolyglutamylated tubulin antibody (Bobinnec et al., 1998). Using HeLa cells stably transfected with centrin-1/GFP to mark centrioles (Piel et al., 2000), we ablated one of the centrosomes at metaphase. Upon the completion of mitosis, such cells divided into a centrosome-containing and an acentrosomal daughter cells. Contrary to what was found when centrosomes were removed from untransformed BSC1 and CV1 cells (Hinchcliffe et al., 2001; Khodjakov and Rieder, 2001), we observed that acentrosomal HeLa cells continue to progress through the cell cycle and reform centrioles de novo.

Results

HeLa cells born without centrosomes progress through the cell cycle and form centrioles de novo

All experiments were conducted in HeLa cells stably transfected with human centrin-1/GFP. This protein accumulates inside the centriole lumen from the earliest stages of centriole formation, which makes it a reliable marker for individual centrioles (Piel et al., 2000). Using the GFP signal as a target, we laser ablated both centrioles (diplosome) associated with one of the two spindle poles during mitosis. At the completion of mitosis, this produces two genetically identical daughter cells: one with and one without a centrosome. Comparative analysis of the two sisters allowed us to differentiate between the effects specific to the centrosome ablation versus potential nonspecific effects of laser irradiation and long-term fluorescence imaging. It is important to emphasize that the laser beam destroys all structures/proteins within an $\sim 0.4\text{--}0.4\text{--}0.6\text{-}\mu\text{m}$ (x-y-z) volume. When we aimed the laser at a centriole, the beam destroyed both the centriole and the PCM associated with the targeted centriole. Thus, ablation

of both centrioles results in the structural and functional destruction of the entire centrosome (Khodjakov et al., 1997, 2000; for review see Khodjakov and Rieder, 2004). However, it is possible to ablate just a single centriole (along with its associated PCM) within a diplosome so that the other centriole (and its PCM) remain intact (see Materials and methods).

We found that complete ablation of one of the two centrosomes in HeLa cells at metaphase or early anaphase did not affect cytokinesis, reconstitution of nuclei, and postmitotic flattening (Fig. 1). Time lapse microscopy revealed that the centrosomal and acentrosomal sisters are morphologically indistinguishable from each other and exhibit similar behavior, which is consistent with our previous observations in CV-1 and PtK₁ cells (Khodjakov et al., 2000; Khodjakov and Rieder, 2001). However, in sharp contrast with nontransformed cells (e.g., CV-1, BSC-1, or PtK₁) that arrest during G₁ in the absence of centrosomes (Hinchcliffe et al., 2001; Khodjakov and Rieder, 2001), HeLa cells born without centrosomes progressed through the cell cycle with normal timing. These cells entered the next mitosis at 31.9 ± 7.1 h ($n = 16$) versus 30.6 ± 7.3 h ($n = 14$) for their centrosomal sisters. To standardize our descriptions of the progression through several consecutive cell cycles for these cells, we will hereafter refer to the completion of the mitosis during which the centrioles were ablated as the “birth” of the cell. After birth, the cells undergo a “first” cell cycle that culminates in the “first mitosis”, and then the “second cell cycle” and “second mitosis,” etc.

Approximately 20–25 h into the first cell cycle, a number of minuscule aggregates of centrin/GFP appeared in the cytoplasm of cells that were born without centrioles. Initially, these aggregates were barely recognizable against the diffuse centrin/GFP background fluorescence (Videos 1 and 2, available at <http://www.jcb.org/cgi/content/full/jcb200411126/DC1>). Their intensity gradually increased until they reached the levels typical for normal centrioles in this cell line (Fig. 2 and Videos 1 and 2). The increase in intensity was usually completed just before or during first mitosis (30–35 h after the cell’s birth). The number of aggregates was variable (from 2 to >10 per cell); however, once the initial aggregates became detectable, their number in an individual cell did not increase over time.

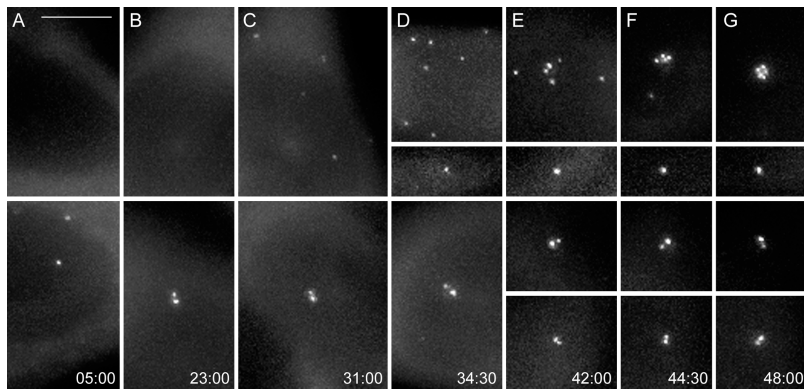


Figure 2. Reformation of centrin/GFP aggregates and their behavior in HeLa cells born without a centrosome. Selected GFP fluorescence frames (maximal-intensity projections) from a multimode time lapse recording (same recording as in Fig. 1). The cell born without centrosome exhibits only diffuse cytoplasmic centrin/GFP localization for ~ 24 h (A and B, top). Then, small centrin/GFP aggregates appear in the cytoplasm (C). These aggregates move continuously in the cytoplasm (see Videos 1 and 2, available at <http://www.jcb.org/cgi/content/full/jcb200411126/DC1>). After mitosis, which occurs at 32 h (Fig. 1 E) one of the progeny inherits seven of these aggregates, whereas the other inherits just one aggregate (D). The seven aggregates continue to move in the cytoplasm for ~ 7 –8 h (E), and then they coalesce into a common structure that remains relatively stationary in the middle of the cell (F and G, and Fig. 11). The centri-

oles in the sister cell that inherited a normal centrosome (bottom) exhibit expected behavior, because they replicate (D) and then are properly distributed between the daughter cells after mitosis (E). Times are shown in hours:minutes. Bar, 5 μ m.

This indicated that the formation of the aggregates in each cell occurred within a relatively short period of time instead of gradually accumulating as the cell progressed through the cell cycle.

Correlative GFP fluorescence light microscopy/serial-section EM analyses revealed that these aggregates are amorphous at the EM level for ~ 5 –10 h after they became recognizable by light microscopy ($n = 2$). Nevertheless, by the time the cells reached first mitosis or the second cell cycle centrin aggregates corresponded to morphologically complete centrioles (Fig. 3) in all cells investigated ($n = 3$). Limited sample size did not allow us to identify intermediate stages of the transition from the amorphous centrin aggregates to complete centrioles in cycling cells. During first mitosis, centrioles did not pair to form diplosomes, but rather they organized spindle poles as individual centrioles (Fig. 3), surrounded by minimal amount of PCM.

De novo-assembled centrioles mature during second cell cycle

In control HeLa cells, the mother and daughter centrioles exhibit dramatically different mobility during early G_1 . Whereas the mother centriole remains relatively stationary in the center of the cell, the daughter moves extensively in the cytoplasm making numerous excursions to the periphery of the cell and returning back to the center. These excursions cease at G_1/S transition (Piel et al., 2000; Video 3, available at <http://www.jcb.org/cgi/content/full/jcb200411126/DC1>).

Our recordings revealed that centrin aggregates also moved extensively in a random fashion throughout first interphase until the cells entered mitosis (Fig. 2 and Videos 1 and 2). During the first mitosis, approximately half of the mitotic cells (11/20) exhibited extra cleavage furrows and produced one mononucleated and one multinucleated daughter cell, which implies the assembly of multipolar spindles in cells with de novo–formed centrioles. Furthermore, we directly observed multipolar mitotic spindle in three cells fixed during first mitosis. Serial section EM reconstruction revealed that centrioles were associated with the spindle poles (Fig. 3).

After completion of first mitosis, which on average was longer in cells born without centrioles (2.9 ± 2.2 h; $n = 13$) than in their centrosomal sisters (2.0 ± 1.9 h; $n = 12$), the de novo–formed centrioles resumed movements that were similar to those exhibited by the centrin aggregates during the previous cell cycle. Then, at 2–10 h after mitosis, all centrioles suddenly coalesced into a relatively stationary complex (Fig. 2, E–F; and Videos 1 and 2). In all cases, the coalescence itself was relatively rapid, as all centrioles came together in < 2 h. Thus, centriole coalescence corresponds to a pronounced change in behavior: from that normally exhibited by the daughter centrioles to the one typical for the mothers. The coalescence of the centrioles always occurred in the second cell cycle.

It has been previously shown that the motilities of the daughter and mother centrioles during G_1 correlate with their

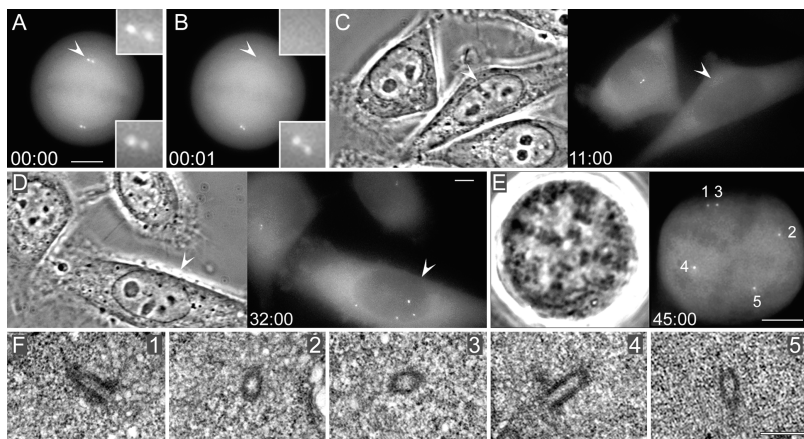


Figure 3. Centrin aggregates formed in cells born without centrosomes become morphologically recognizable as centrioles when the cell enters mitosis. (A and B) Fluorescence images of a metaphase cell before (A) and after (B) laser ablation of one of the two centrosomes (A and B, compare arrowheads). Insets are shown at a higher magnification. (C–E) The cell born without a centrosome (C and D, arrowheads) forms prominent centrin aggregates, enters mitosis, and forms a multipolar mitotic spindle. The left image in each panel shows phase-contrast microscopy; the right images show centrin/GFP fluorescence. (F) Serial section EM analysis of this cell reveals that each of the centrin aggregates corresponds to a single centriole, surrounded by a small amount of pericentriolar material (1–5; selected sections from a full series of 100-nm sections). Time is shown in hours:minutes. Bars: (A–E) 5 μ m; (F) 500 nm.

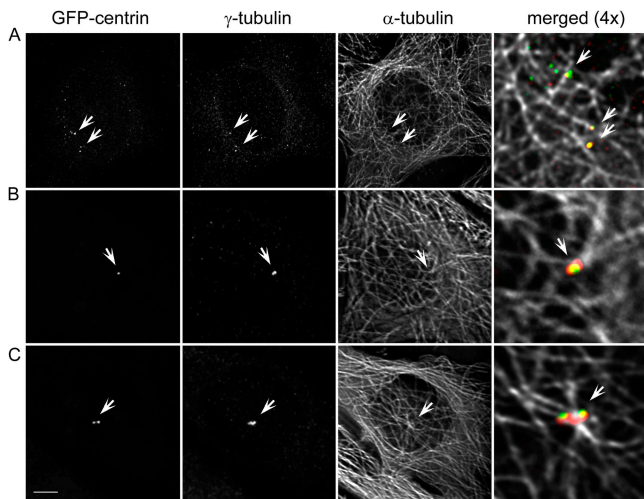


Figure 4. Centrin aggregates are not associated with microtubules during the first cell cycle, but become positioned inside of microtubule foci after they coalesce into a common structure in the second cell cycle. (A) GFP/centrin, γ -tubulin, and α -tubulin distribution in a cell fixed during first cell cycle (\sim 49 h after centrosome ablation and 24 h after formation of detectable centrin aggregates). Although some of the centrin/GFP aggregates also contain γ -tubulin, none of them is associated with microtubule foci (arrows). (B and C) Two progeny of a cell born without a centrosome that were fixed in the second cell cycle, after the coalescence of the de novo-formed centrioles (\sim 48 h after centrosome ablation; 20 h after formation of centrin aggregates; and 15 h after second mitosis). In contrast to the centrin aggregates during the first cell cycle (A), de novo-formed centrioles after mitosis reside inside of microtubule foci and are associated with large amount of γ -tubulin (arrows). Bar, 10 μ m. Maximal-intensity projections.

ability to organize microtubule networks. Although both daughter and mother centrioles are capable of nucleating similar numbers of microtubules, only the mother can organize microtubules into a typical radial array (Piel et al., 2000). As a result, mother centrioles always reside inside of microtubule foci, whereas the daughters, at least in some cell types (e.g., HeLa and L-929), are not associated with microtubule asters (Piel et al., 2000). We investigated at which point the de novo-formed centrioles become associated with microtubule foci. Immunofluorescence analysis revealed that, not surprisingly, the moving centrin aggregates/centrioles of the first interphase were not associated with microtubules, even though some of them were

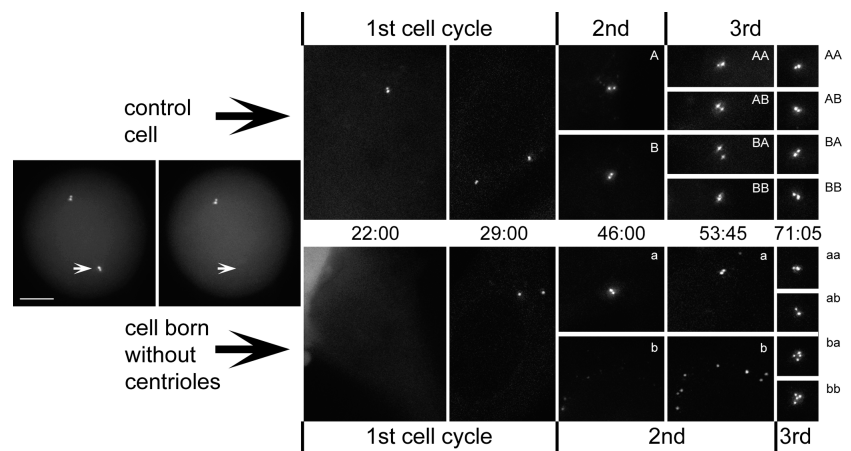
associated with bona fide PCM components, such as γ -tubulin (Fig. 4 A). During the first cell cycle, the interphase microtubule array in cells born without centrioles did not converge on common focal points and were instead randomized, showing only loose concentration at the perinuclear region. Importantly, this difference in microtubule organization was observed even in those cells where the duration of first cell cycle was for some reason prolonged, something that occurs with equal frequency in cells born with and without centrosomes.

In contrast, after coalescence in the second cell cycle, all centrioles were found to be associated with prominent PCM and reside at the focus of microtubule array (Fig. 4, B and C). Although microtubules in HeLa cells are not prominently radial, the foci associated with the de novo-formed centrioles were very similar to those in the surrounding control cells. Even in those cells that by chance inherited only one centriole, this centriole was able to organize a microtubule focus (Fig. 4 B). The appearance of the centrosome in those cells, that by chance inherited two centrioles, was very similar to that in control cells during late G₁ (Fig. 4 C). These observations revealed that, while formation of the morphologically complete centrioles occurs during the first cell cycle, they become competent microtubule-organizing centers only during G₁ of the second cell cycle.

The difference between mature (mother) and immature (daughter) centrioles is not limited to their ability to organize microtubules. An important step in the maturation process is to gain the ability to give birth to a new daughter centriole (for conceptual review see Mazia, 1987). Thus, if the de novo-assembled centrioles become mature during the second cell cycle, then they should begin to replicate in a normal fashion. We tested this prediction by following the progeny of cells born without centrioles with continuous time lapse microscopy over three consecutive cell cycles. We were able to obtain full three-cell cycle-long pedigrees for two cells born without centrioles. Analyses of these pedigrees revealed several important features of the centriole cycle. First, we found that centrioles formed de novo replicate in the second cell cycle (Fig. 5, cell a, which fortuitously inherited two de novo-formed centrioles, and its progeny aa and ab). Second, we found that the de novo pathway becomes active whenever the resident centrioles disappear from the cell. This was evident from those cases in

Figure 5. Pedigree of a cell born without centrosome.

In this particular experiment, the acentrosomal cell formed two centrioles during the first cell cycle (compare 22:00 with 29:00). When this cell underwent mitosis, both de novo-formed centrioles were distributed to one of the two progeny (a), leaving the other one acentrosomal (b). This cell activated the de novo pathway, which now resulted in the formation of eight new centrioles (b, compare 46:00 with 53:45). During third mitosis these 8 centrioles were equally distributed between the two progeny (ba and bb). Cell a, which inherited two de novo-formed centrioles as the result of the second mitosis, replicated these centrioles during the second cell cycle so that both progeny of this cell (aa and ab) inherited two centrioles (one mother and one daughter). Control cell (sister of the cell born without a centrosome) and its progeny exhibited the expected orderly replication of centrioles in both first and second cell cycles. Time is shown in hours:minutes. Bar, 5 μ m.



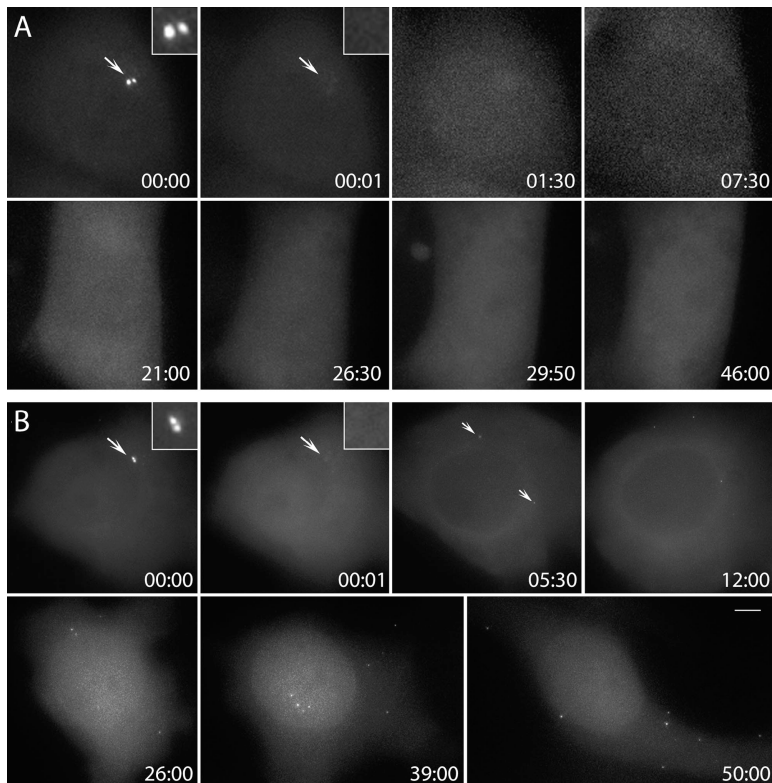


Figure 6. Centriole de novo formation occurs in HeLa cells arrested in S but not in G₁. (A) Resident centrosome was ablated (arrows, compare 00:00 and 00:01) in a cell pretreated with 5 μ M lovastatin for \sim 15 h. Time lapse recording of this cell revealed no formation of centrin/GFP aggregates for 46 h. (B) Similar procedure to A was followed, except this cell was pretreated with 2 mM hydroxyurea. Time lapse recording revealed that \sim 5 h after ablation of the resident centrioles centrin/GFP, aggregates formed in the cytoplasm (arrows, 05:30). These aggregates moved continuously in the cytoplasm while their intensity gradually increased (05:30–50:00). Time is shown in hours:minutes. Bar, 5 μ m.

which all the de novo–formed centrioles were distributed to only one of the progeny (Fig. 5, cell a; and Figs. S1 and S2). As a result, the sister cell was born without a centrosome (Fig. 5, cell b), not because of laser ablation, but because of centriole misdistribution. This cell exhibited de novo assembly of eight centrioles that were later distributed in a four-and-four fashion between the two progeny in the next mitosis (Fig. 5, cell b and its progeny ba and bb). It is noteworthy that this mitosis was multipolar; however, because of retraction of one of the cytokinesis furrows, it resulted in the formation of two cells—one mononucleated and one binucleated (not depicted). Thus, de novo–assembled centrioles become completely mature in the next cell cycle after their assembly.

De novo centriole assembly occurs during the S phase

Thus far, our data revealed that formation of a mature centriole takes place over two consecutive cell cycles in normally cycling cells. However, it remained unclear whether this was simply a time-dependent process or if progression through the cell cycle is required for centriole formation/maturation. To address

this question, we conducted centriole ablations in cells arrested in G₁ with lovastatin or S with hydroxyurea.

We found that formation of centrin aggregates did not occur after ablating resident centrioles in cells arrested during G₁ (Fig. 6 A; $n = 5$). In contrast, cells arrested in S (Fig. 6 B; $n = 5$) consistently formed numerous centrin aggregates after the resident centrosome was laser ablated. These dots gradually increased in intensity until they were indistinguishable from normal centrioles. The kinetics of this intensity increase was similar to those observed in the cycling cells during the first cell cycle. EM analysis revealed that centrin aggregates developed into morphologically recognizable centrioles in S-arrested cells ($n = 2$). In one cell, we found that some centrin aggregates corresponded to structures that appeared to be intermediate stages of centriole formation. EM tomography reconstructions of three of the centrin aggregates in this cell revealed that one of the aggregates corresponded to an electron dense amorphous cloud, with just two microtubule blades present within the cloud. The other two centrin dots corresponded to more completed, although still abnormal, centrioles. These structures contained four microtubule blades in one case and six to seven

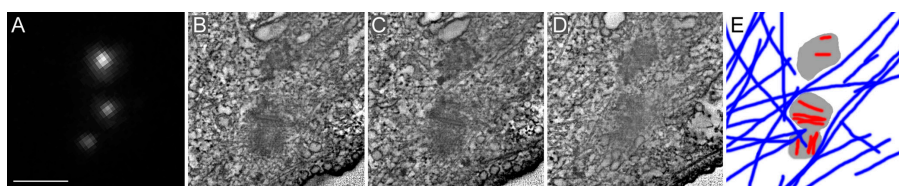


Figure 7. Intermediate stages of centriole formation in S-arrested cells. Similar procedure to Fig. 6 B was performed, except this cell was fixed 24 h after ablating the resident centrosome. (A) GFP fluorescence revealed that several prominent centrin/GFP aggregates had formed in the cell. (B–D) Individual 3.2-nm-thick slices from the tomogram of a 100-nm-thick section revealed that some of

these aggregates correspond to centriole-like structures that appear to be at different stages of assembly. (E) Tracing of microtubules (blue) centriolar blades and electron-opaque material from the tomogram. Note that while there are multiple microtubules, they do not converge on the forming centrioles. Bar, 500 nm.

in the other; however, the triplet blades were not properly organized into closed cylinders (Fig. 7 and Video 4, available at <http://www.jcb.org/cgi/content/full/jcb200411126/DC1>).

Fluorescence time lapse microscopy of centrin aggregates/centrioles formed in S-arrested cells revealed that they move continuously in the cytoplasm in the same fashion as centrin aggregates/immature centrioles do in cycling cells during the first interphase (Fig. 6 B and Video 5, available at <http://www.jcb.org/cgi/content/full/jcb200411126/DC1>). This motion continued for as long as we were able to follow S-arrested cells (~50 h), and the aggregates never coalesced into a common complex. In light of our EM data, these observations indicate that the complete process of centriole biogenesis, but not maturation, can proceed to completion during the S phase.

De novo centriole formation is inhibited by the presence of a single resident centriole

Our observations indicated that de novo assembly of centrioles in HeLa cells occurs whenever resident centrioles disappear from the cell. The means in which the centrioles vanish from the cell do not appear to be important, for we observed de novo centriole assembly after ablation of resident centrioles as well as in cells that lost their centrioles via misdistribution during mitosis (Fig. 5). The fact that de novo centriole assembly pathway activates whenever resident centrioles are missing implies that cells possess a mechanism that somehow senses the presence of centrioles. In this respect, it is important to determine whether this mechanism monitors the presence of a mature (mother) centriole or whether it is satisfied by any centriole present in the cell. To address this issue, we laser ablated just one mother centriole within the diplosome at a spindle pole during mitosis. As mother centrioles contain greater amounts of centrin than the daughters, the relative intensity of the GFP signal allowed us to distinguish the mother centriole from the daughter in live cells (Fig. 8; Piel et al., 2000, 2001). As a result of such an operation, one daughter cell is born with just one immature centriole. We reasoned that, if inhibition of the de novo pathway requires the presence of the mother centriole, cells born with one immature centriole would exhibit the de novo assembly of multiple centrioles.

Time lapse recordings of cells that inherited just one immature centriole revealed that all ($n = 3$) entered the subsequent mitosis with only a single diplosome, which was formed as the result of replication of the resident centriole (Fig. 8). We did not detect any signs of the de novo pathway activity. The duration of the cell cycle appeared not affected in monocentricular cells (Fig. S1, available at <http://www.jcb.org/cgi/content/full/jcb200411126/DC1>), which was not surprising in light of our data on complete centrosome ablation. Importantly, the single diplosome present in these cells associated with only one of the two spindle poles (Fig. S2) and thus one of the two cells formed as the result of first mitosis was born with normal centriole complement, while its sister lacked centrioles completely. Whereas cells that inherited the diplosome proceeded with orderly centriole replication in the ensuing cell cycle, their sisters born without centrioles exhibited de novo assembly of a variable number of centrioles (Fig. 8 and Fig. S1).

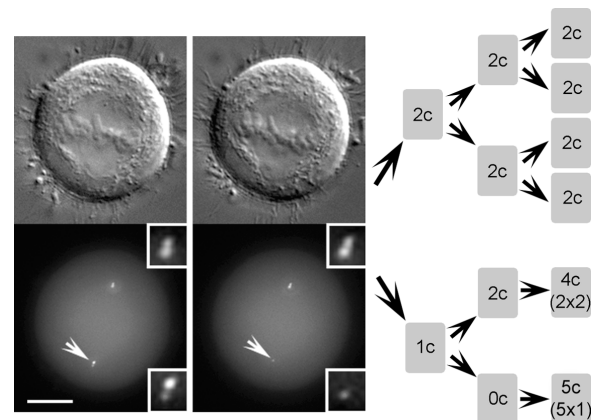


Figure 8. Pedigree of a cell born with only one (daughter) centriole. In this cell, just one (mother) centriole within a diplosome was ablated (white arrows; insets present centrioles at a higher magnification). As a result, after the end of mitosis, one daughter cell was born with normal centrosome, but the other one inherited only one (daughter) centriole. This centriole replicated once during the first cell cycle, and the resulting diplosome was distributed to one of the progeny during second mitosis. As a result, one of the progeny now inherited a normal centrosome (one daughter and one mother centriole), whereas the other one was born without a centrosome. This cell eventually formed five centrioles de novo. Progeny of the control cell (sister of the one born without centriole) exhibited expected centriole replication pattern.

De novo centriole formation is not a consequence of laser fragmentation of the resident centrosome

One formally possible complication of the laser ablation approach to centrosome inactivation is that the laser pulses may cause fragmentation of the centrioles and/or the PCM rather than their complete destruction. If so, the de novo assembly of centrosomes might simply reflect the seeding of centrosomes from tiny preexisting fragments of the original centrosome. To unequivocally test this possibility, we used glass needle microsurgery to remove centrosomes from HeLa cells and to determine whether centrioles would form de novo. Needle microsurgery is effective in completely removing the centrosome from interphase BSC-1 fibroblasts (Maniotis and Schliwa, 1991; Hinchcliffe et al., 2001), and this method cannot induce centrosome fragmentation.

We used the GFP centrin signal to identify cells with two centrioles (G_1) that were located away from the nucleus. Such cells were then cut with a glass needle so that a piece of cytoplasm containing the centrosome was separated from the rest of the cell (Fig. S3, available at <http://www.jcb.org/cgi/content/full/jcb200411126/DC1>; also see Hinchcliffe et al., 2001). We then followed each karyoplast by phase-contrast video microscopy for 22–72 h; at the end of the video records, we collected three-dimensional (3-D) fluorescence images. Nine karyoplasts were followed through the first division, and seven were fixed 9–12 h after its completion. The duration of mitosis was ~2 h (range 1–6), which is in good agreement with the duration of the first mitosis in cells after laser ablation of centrosomes. Most karyoplasts formed more than one furrow during cytokinesis, which once again was reminiscent of the cytokinesis pattern in cells after centrosome laser ablation, and implied that

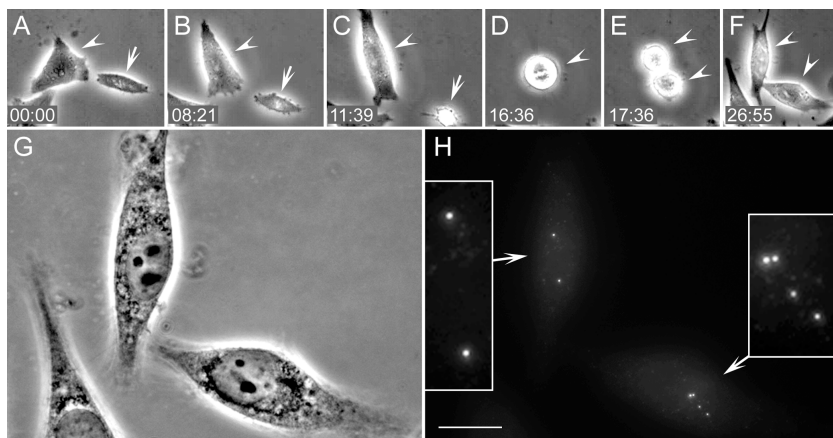


Figure 9. HeLa cells progress through the cell cycle and form centrioles de novo after removal of the resident centrosome by needle microsurgery. A large piece of cytoplasm containing both centrioles (i.e., cytoplasm; A–C, arrow) was separated from the rest of the cell by a microneedle (see Fig. S3, available at <http://www.jcb.org/cgi/content/full/jcb200411126/DC1>). The nucleus-containing karyoplast (A–F, arrowheads) entered mitosis ~ 16 h after the operation (D). The division resulted in the formation of two daughter cells (E) that were followed for an additional 9 h, and then transferred onto a higher magnification microscope. Multimode phase-contrast (G) and 3-D fluorescence (H) imaging revealed that one of the daughter cells contained 2 and the other one 4 centrioles. Insets in H present centrioles at a higher magnification. Bar, 10 μ m.

the mitotic spindle in karyoplasts was multipolar. However, extra furrows regressed and all nine karyoplasts ultimately divided just two daughter cells. All daughter karyoplasts contained a variable number (1–5 per cell) of bright centrin/GFP aggregates indistinguishable from those observed after laser ablations (Fig. 9). Importantly, the number of centrin foci was different between daughter karyoplasts, indicating that the distribution of these structures during mitosis was random, as observed for centrioles formed de novo after laser ablation.

The progeny of two karyoplasts were followed through the second cell cycle, second mitosis, and fixed at ~ 12 h into the third cell cycle. Each of these cells contained bright centrin aggregates clustered together in a common complex, as expected for de novo–formed centrioles after the maturation (unpublished data). Control amputations of large portions of cytoplasm, not containing centrioles, did not alter cell cycle progression, the normal pattern of centriole duplication, or induced the formation of supernumerary centrin foci (unpublished data).

Discussion

The centrosome is not required for cell cycle progression in HeLa cells

CV-1, BSC-1, and PtK₁ cells, born without a centrosome, arrest in G₁ and do not assemble centrioles de novo (Khodjakov and Rieder, 2001; Hinchcliffe et al., 2001). In contrast, we now find that acentrosomal HeLa cells progress through the cell cycle with normal timing and form a variable number of centrioles de novo. The question then arises as to whether HeLa cells are capable of assembling centrioles in G₁, which then allows progression into S phase, or whether they lack mechanisms blocking cell cycle progression in the absence of centrioles. Our observation that HeLa cells arrested during G₁ with lovastatin fail to form centrioles support the latter scenario. Just like in other cell types (Marshall et al., 2001; Khodjakov et al., 2002), de novo centriole assembly in HeLa occurs only during S phase. Thus, HeLa cells progress through G₁ without centrioles.

So far, we observed G₁ arrest in response to centrosome disappearance only in nontransformed cell lines that are p53-positive, substrate-dependent, and originate from normal tissue.

In contrast, HeLa cells originate from cervical adenocarcinoma, can be grown in suspension, and have functionally suppressed p53 and Rb as well as deregulated cyclin A expression (for review see zur Hausen, 1996). Thus, the ability or inability to progress through G₁ in the absence of centrioles appears to correlate with whether the cells are normal or transformed, respectively.

In any case, the important principle emerging from this work is that G₁ progression in mammalian somatic cells does not absolutely require a centrosome; neither the centrosome nor any of its activities are an integral part of the pathways that take a cell through G₁ into S phase. Such a “relief of dependency” (Hartwell and Weinert, 1989) implies the existence of a surveillance mechanism (i.e., a checkpoint) that monitors a centrosome-dependent function in normal cells as they enter G₁.

Centrioles possess an activity that represses the de novo pathway

We find that de novo centriole assembly does not take place when there is a single resident centriole in the cell; it occurs only upon the disappearance of all resident centrioles regardless of the means used to eliminate them (i.e., after ablating the resident centrosome with the laser, after removing it from the cell with a micro-needle, or upon mis-distribution of centrioles during mitosis yielding an acentriolar cell). Thus, centrioles possess an activity that suppresses the de novo pathway (Marshall et al., 2001).

This activity may contribute to the way the cell exercises precise spatial, temporal, and numerical control over centriole duplication in the normal cell. Perhaps, the proximal end of mother centrioles contains a “docking site” that stabilizes and accelerates conversion from a centrin aggregate (precentriole) into a centriole. In this respect, we often detected accumulation of a number of minuscule centrin aggregates in control cells during interphase. However, within a few hours of their formation, these aggregates disappeared (unpublished data). Thus, the formation of precentrioles might always occur via a de novo mechanism and is not under precise numerical control. However, only those precentrioles that associate with the mature resident centrioles are stabilized and elaborate triplet microtubules to become daughter centrioles. This mechanism

readily explains why centrioles are normally not capable of reduplication within a single cell cycle (Wong and Stearns, 2003) because the stabilization site on the mature centriole may not become available again until the cell undergoes mitosis.

Centriole cycle and the cell cycle are coordinated by distinct events in S and G₁

Our finding of de novo centriole formation in cycling cells allowed us to follow the development of centrioles from birth to maturity in the absence of resident mother centrioles whose activities could potentially influence the maturation of the daughters. We observed three distinct stages of the centriole development: (1) formation of centrin aggregates (precentrioles); (2) assembly of the 9 triplet microtubules to form morphologically complete centrioles; and (3) centriole maturation (Fig. 10). We find that formation of precentrioles is first manifested as aggregation of centrin, a protein present in the centriolar lumen and required for centriole replication (Paoletti et al., 1996; Mittenborn et al., 1997). Centrin is abundant in cells and only <10% of the total centrin is associated with the centrosome (Paoletti et al., 1996). Since centrin shows no tendency to aggregate when overexpressed, it is likely that the precentriole formation is seeded by other components such as the centrin-binding protein Sfi1p (Kilmartin, 2005).

The transformation of precentrioles into morphologically recognizable centrioles is a time-dependent process that runs to completion even when the cell is arrested in S phase by hydroxyurea. When cells progress through S phase with normal kinetics, morphologically recognizable centrioles are not seen until cells approach or enter mitosis. However, we note that, in the normal cell cycle, morphologically recognizable daughter centrioles are consistently found significantly earlier, during early the S period (Vorobjev and Chentsov, 1982; Kuriyama et al., 1986). This temporal difference suggests that the normal association of precentrioles with the proximal ends of mother centrioles accelerates the assembly of the barrel of nine triplet microtubules.

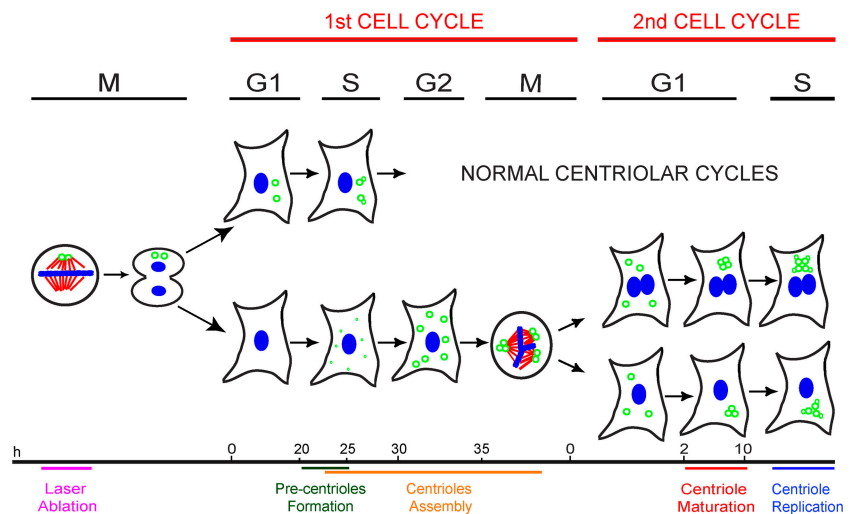
The third, or maturation stage, of the centriole development corresponds to a transition in the structural and functional

properties of the centriole. The process involves recruitment of additional proteins, such as ninein (Piel et al., 2000; Abal et al., 2002), elaboration of appendages, and is functionally manifested as a dramatic change in the mobility and microtubule anchoring capability of the centriole. While daughter centrioles continuously move in the cytoplasm and are not associated with microtubules, the mothers remain relatively stationary in the center of a microtubule focus (Piel et al., 2000). We find that the maturation of the newly formed centrioles occurs only during G₁ of the next (after centriole formation) cell cycle. It is important to emphasize, that centriole maturation is not simply a gradual time-dependent process, as de novo-assembled centrioles remain functionally immature for as long as the HeLa cells are arrested in S phase of the cycle in which these centrioles are assembled. We also observed no centrosome maturation in those cells that were naturally delayed in their progression through the cell cycle. Only after completion of mitosis do the centrioles coalesce into an immobile complex and organize a radial microtubule array. Thus, centriole assembly and maturation are coordinated with the cell cycle by distinct events during S and G₁ respectively.

The de novo pathway and cancer

Cancerous cells often possess supernumerary centrosomes, a phenomenon known as “centrosome amplification.” The presence of extra centrosomes greatly increases the probability that such cells will assemble multipolar spindles during mitosis and exhibit genomic instability though unequal chromosome distribution (for reviews see Pihan et al., 1998; Brinkley and Goepfert, 1998). Centrosome amplification has been attributed to cleavage failure and/or centrosome reduplication in a given cell cycle (for reviews see Brinkley and Goepfert, 1998; Pihan et al., 1998; Brinkley, 2001; Nigg, 2002; Tarapore and Fukasawa, 2002). Our observations indicate that the de novo formation of centrioles could also contribute to centrosome amplification. Intriguingly, our data suggest that the consequences of the loss of resident centrosome are dramatically different for normal versus transformed cells because only the latter cells escape G₁ arrest in the absence of centrioles. Thus, if

Figure 10. **Timeline of centrosome reformation in HeLa cells.** When a cell is born without centrioles, it continues to progress through the cell cycle with normal kinetics. When cells enter S phase, multiple aggregates of centrin (precentrioles, small green dots) form. These precentrioles transform into morphologically complete centrioles (green open circles) by the time the cell enters its first mitosis. However, de novo-formed centrioles do not mature centrosomes until the ensuing G₁ in the second cell cycle. As cell enters the second cell cycle S phase, de novo-formed centrioles replicate and normal centriolar cycles resume.



centrosome misdistribution during mitosis produces an acentriolar daughter cell, then normal cells would remain arrested during G₁, however, in transformed cells activation of the de novo pathway will directly result in centrosome amplification through the assembly a multiple centrioles in these cells.

Materials and methods

Cell culture and drug treatments

HeLa-C1 (Piel et al., 2000) cells were provided by M. Bornens (Institut Curie, Paris, France). Cells were grown in antibiotic-free DME supplemented with 10% FBS (HyClone). Cells were maintained in a humidified incubator at 37°C in 5% CO₂ atmosphere.

2 mM hydroxyurea, 10 μM aphidicolin, or 5 μM lovastatin were added to cells ~15 h before laser microsurgery. All reagents were purchased from Sigma-Aldrich. For laser microsurgery experiments, cells that were grown on coverslips were mounted in Rose chambers in phenol-free L15 medium supplemented with 10% FBS. During experiments, cells were maintained at 37°C either with custom-built Rose chamber heaters.

Laser microsurgery

Laser ablation of centrosomes was performed as described previously (Khodjakov et al., 2000, 2002; Khodjakov and Rieder, 2001). In brief, collimated 7-ns pulses of 532-nm light from Nd:YAG laser (Surelite II) were steered through the lower epi-port of a microscope (model TE200E; Nikon), equipped with electronically controlled X-Y stage (Ludl) and UniBlitz shutters (Vincent Associates). The beam was focused 60 × 1.4 NA PlanApo lens that was also used for observations. It takes ~10 laser pulses (1 s) to destroy the centrosome. The system was driven by IP Lab software (Scanalytics), and the images were recorded on the cooled CCD camera (CoolSnap HQ; Photometrics). Images were acquired at 50–200-ms exposures.

Glass needle microsurgery

Glass needle microsurgery and time lapse phase-contrast recording were conducted essentially as described in Hinchcliffe et al. (2001). Karyoplasts were followed until 12 h after the first mitosis or until 12 h after the second mitosis, at which points the cultures were fixed and the state of the centrosome in the karyoplasts characterized by 3-D GFP/immunofluorescence.

Long-term imaging

After laser ablation of the centrosome, the position of the experimental cell was marked with a diamond-tip objective scribe (Carl Zeiss MicroImaging, Inc.). This allowed us to reidentify the cell when the chamber was shuttled between high- and low-power microscopes as well as after fixing the cell for subsequent EM or immunofluorescence analyses.

We used two different strategies to record long-term (up to 85-h) time lapse sequences. In some experiments, phase-contrast time lapse images were recorded at lower magnification using a microscope (model TMS; Nikon) equipped with a video camera. This microscope was stationed in a temperature-controlled room stabilized at 37°C. Every few hours, the chamber was transferred onto a high-power microscope to collect 3-D fluorescence images (see next section), and then immediately returned onto the low-power microscope. Although this approach yielded only a few GFP fluorescence data points per recording, it was least stressful for the cells.

The second strategy was to record continuous multimode time lapses with high-power (60 × 1.4 or 100 × 1.4 PlanApo lenses). These recordings were done in near simultaneous phase-contrast (or DIC)/fluorescence mode at 30-min intervals on one of our multimode imaging workstations (see next section). Fluorescence images were collected as Z series (17 optical planes separated by 0.5 μm for each time point). The exposure times were 300 or 500 ms for each plane. Maximal intensity projections were then computed from the 3-D datasets and were contrast manipulated in Photoshop.

Fluorescence microscopy

Stacks of fluorescence images (as z-series) were collected using Nikon Eclipse TE200 or TE300 inverted microscopes, both equipped with filter wheels (Ludl), piezo Z-positioners (Physik Instrumente, Germany), and electronically controlled shutters (Vincent Associates, Rochester, NY). Images were captured with either CoolSnap HQ (Photometrix, Tucson, AZ) or Orca II (Hamamatsu) cooled-CCD cameras. Each microscope was driven by Isee software (Isee Imaging, Raleigh, NC).

Immunostaining

Cells were fixed in 1% glutaraldehyde for 30 min at room temperature and post-fixed with cold methanol for 2 min. The following antibodies were used: mouse monoclonal anti-α-tubulin DM1α and anti-γ-tubulin GTU-88 (both purchased from Sigma-Aldrich). Secondary antibodies (TRITC conjugated) were purchased from Sigma-Aldrich. DNA was counterstained with 5 μg/ml Hoechst 33342.

Electron microscopy

Fixation, embedding, and serial sectioning for EM were performed according to standard procedures (Rieder and Cassels, 1999). Double tilt EM tomography was performed as described in McEwen and Marko (1999). In brief, 20-nm colloidal gold particles were attached to a single surface of the section to serve as fiducial markers for subsequent image alignment. A double tilt tomographic dataset was recorded using an electron microscope (model F20; Technai) operated at 200 kV. Images were captured based on a cosine 2° scheme over ±70° range using a 2k × 2k CCD camera (Gatan) at a pixel size of 3.2 nm. IMOD was used for image alignment and tomographic computations (<http://bio3d.colorado.edu/imod>).

Online supplemental materials

Fig. S1 shows mitosis in a cell with only one diplosome. Fig. S2 shows removal of centrosome by glass needle microsurgery Fig. S3 shows selected frames from the time lapse recording of the cell depicted in Fig. 8. Video 1 shows the behavior of de novo–formed centrioles during the first and second cell cycles in HeLa cells. Video 2 provides another example of the de novo–formed centriole behavior during the first and second cell cycles in HeLa cells. Video 3 presents the behavior of resident centrioles during normal cell cycle in HeLa cells. Video 4 presents a walk-through the tomographic reconstruction of de novo–forming centrioles. Video 5 shows the behavior of centrioles formed de novo in a HeLa cell arrested in S with hydroxyurea. Online supplemental material is available at <http://www.jcb.org/cgi/content/full/jcb200411126/DC1>.

We thank Dr. Michel Bornens for HeLa cells expressing centrin-1/GFP and Ms. Kristin Vandenberg for assistance with electron tomography. We acknowledge the use of Wadsworth Center's EM core facility. We also thank Dr. Conly Rieder for helpful discussions and encouragement during the course of this work, and for his critique of the manuscript.

This work was supported by grants from the National Institutes of Health (GM59363 to A. Khodjakov; GM30758 to G. Sluder; and GM06627 and National Science Foundation MCB0110821 to B.F. McEwen). Assembly of the laser microsurgery system was supported in part by Marine Biological Lab/Nikon fellowship to A. Khodjakov.

Submitted: 22 November 2004

Accepted: 19 January 2005

References

- Abal, M., M. Piel, V. Bouckson-Castaing, M.M. Mogensen, J.-B. Sibarita, and M. Bornens. 2002. Microtubule release from the centrosome in migrating cells. *J. Cell Biol.* 159:731–737.
- Bobinnec, Y., A. Khodjakov, L.M. Mir, C.L. Rieder, B. Edde, and M. Bornens. 1998. Centriole disassembly in vivo and its effect on centrosome structure and function in vertebrate cells. *J. Cell Biol.* 143:1575–1589.
- Brinkley, B.R. 2001. Managing the centrosome numbers game: from chaos to stability in cancer cell division. *Trends Cell Biol.* 11:18–21.
- Brinkley, B.R., and T.M. Goepfert. 1998. Supernumerary centrosomes and cancer: Boveri's hypothesis resurrected. *Cell Motil. Cytoskeleton.* 41:281–288.
- Hartwell, L.H., and T.A. Weinert. 1989. Checkpoints: controls that ensure the order of cell cycle events. *Science.* 246:629–634.
- Hinchcliffe, E.H., F.J. Miller, M. Cham, A. Khodjakov, and G. Sluder. 2001. Requirement of a centrosomal activity for cell cycle progression through G₁ into S phase. *Science.* 291:1547–1550.
- Kallenbach, R.J., and D. Mazia. 1982. Origin and maturation of centrioles in association with the nuclear envelope in hypertonic-stressed sea urchin eggs. *Eur. J. Cell Biol.* 28:68–76.
- Khodjakov, A., and C.L. Rieder. 2001. Centrosomes enhance the fidelity of cytokinesis in vertebrates and are required for cell cycle progression. *J. Cell Biol.* 153:237–242.
- Khodjakov, A., and C.L. Rieder. 2004. A synergy of technologies: using green fluorescent protein tagging and laser microsurgery to study centrosome function and duplication in vertebrates. *In Centrosome in Development*

- and Disease. E.A. Nigg, editor. Wiley-VCH, Weinheim. 191–210.
- Khodjakov, A., R.W. Cole, and C.L. Rieder. 1997. A synergy of technologies: combining laser microsurgery with green fluorescent protein tagging. *Cell Motil. Cytoskeleton*. 38:311–317.
- Khodjakov, A., R.W. Cole, B.R. Oakley, and C.L. Rieder. 2000. Centrosome-independent mitotic spindle formation in vertebrates. *Curr. Biol.* 10:59–67.
- Khodjakov, A., C.L. Rieder, G. Sluder, G. Cassels, O.C. Sibon, and C.L. Wang. 2002. De novo formation of centrosomes in vertebrate cells arrested during S phase. *J. Cell Biol.* 158:1171–1181.
- Kilmartin, J.V. 2003. Sfi1p has conserved centrin-binding sites and an essential function in budding yeast spindle pole body duplication. *J. Cell Biol.* 162:1211–1221.
- Kuriyama, R., S. Dasgupta, and G.G. Borisy. 1986. Independence of centriole formation and initiation of DNA synthesis in Chinese hamster ovary cells. *Cell Motil. Cytoskeleton*. 6:355–362.
- Maniotis, A., and M. Schliwa. 1991. Microsurgical removal of centrosomes blocks cell reproduction and centriole generation in BSC-1 cells. *Cell*. 67:495–504.
- Marshall, W.F., Y. Vucica, and J.L. Rosenbaum. 2001. Kinetics and regulations of de novo centriole assembly: implications for the mechanism of centriole duplication. *Curr. Biol.* 11:308–317.
- Mazia, D. 1987. The chromosome cycle and the centrosome cycle in the mitotic cycle. *Int. Rev. Cytol.* 100:49–92.
- McEwen, B.F., and M. Marko. 1999. Three-dimensional transmission electron microscopy and its application to mitosis research. *Methods Cell Biol.* 61:81–111.
- Middendorp, S., A. Paoletti, E. Schiebel, and M. Bornens. 1997. Identification of a new mammalian centrin gene, more closely related to *Saccharomyces cerevisiae* CDC31 gene. *Proc. Natl. Acad. Sci. USA*. 94:9141–9146.
- Moritz, M., M.B. Braunfeld, J.W. Sedat, B. Alberts, and D.A. Agard. 1995. Microtubule nucleation by gamma-tubulin-containing rings in the centrosome. *Nature*. 378:638–640.
- Nigg, E.A. 2002. Centrosome aberrations: cause or consequence of cancer progression? *Nat. Rev. Cancer*. 2:815–825.
- Palazzo, R.E., E. Vaisberg, R.W. Cole, and C.L. Rieder. 1992. Centriole duplication in lysates of *Spisula solidissima* oocytes. *Science*. 256:219–221.
- Paoletti, A., M. Moudjou, M. Paintrand, J.L. Salisbury, and M. Bornens. 1996. Most of centrin in animal cells is not centrosome-associated and centrosomal centrin is confined to the distal lumen of centrioles. *J. Cell Sci.* 109:3089–3102.
- Piel, M., P. Meyer, A. Khodjakov, C.L. Rieder, and M. Bornens. 2000. The respective contributions of the mother and daughter centrioles to centrosome activity and behavior in vertebrate cells. *J. Cell Biol.* 149:317–330.
- Piel, M., J. Nordberg, U. Euteneuer, and M. Bornens. 2001. Centrosome-dependent exit of cytokinesis in animal cells. *Science*. 291:1550–1553.
- Pihan, G.A., A. Purohit, J. Wallace, H. Knecht, B. Woda, P. Quesenberry, and S.J. Doxsey. 1998. Centrosome defects and genetic instability in malignant tumors. *Cancer Res*. 58:3974–3985.
- Rieder, C.L., and G.G. Borisy. 1982. The centrosome cycle in PtK₂ cells: asymmetric distribution and structural changes in the pericentriolar material. *Biol. Cell*. 44:117–132.
- Rieder, C.L., and G. Cassels. 1999. Correlative light and electron microscopy of mitotic cells in monolayer cultures. *Methods Cell Biol.* 61:297–315.
- Rieder, C.L., S. Faruki, and A. Khodjakov. 2001. The centrosome in vertebrates: more than a microtubule-organizing center. *Trends Cell Biol.* 11:413–419.
- Riparbelli, M.G., and G. Callaini. 2003. *Drosophila* parthenogenesis: a model for de novo centrosome assembly. *Dev. Biol.* 260:298–313.
- Salisbury, J.L., C.M. Whitehead, W.L. Lingle, and S.L. Barrett. 1999. Centrosomes and cancer. *Biol. Cell*. 91:451–460.
- Schnackenberg, B.J., A. Khodjakov, C.L. Rieder, and R.E. Palazzo. 1998. The disassembly and reassembly of functional centrosomes *in vitro*. *Proc. Natl. Acad. Sci. USA*. 95:9295–9300.
- Suh, M.R., J.W. Han, Y.R. No, and J.H. Lee. 2002. Transient concentration of a γ -tubulin-related protein with a pericentrin-related protein in the formation of basal bodies and flagella during the differentiation of *Naegleria gruberi*. *Cell Motil. Cytoskeleton*. 52:66–81.
- Szollosi, D., P. Calarco, and R.P. Donahue. 1972. Absence of centrioles in the first and second meiotic spindles of mouse oocytes. *J. Cell Sci.* 11:521–541.
- Szollosi, D., and J.P. Ozil. 1991. De novo formation of centrioles in parthenogenetically activated, diploidized rabbit embryos. *Biol. Cell*. 72:61–66.
- Tarapore, P., and K. Fukasawa. 2002. Loss of p53 and centrosome hyperamplification. *Oncogene*. 21:6234–6240.
- Vorobjev, I.A., and Y.S. Chentsov. 1982. Centrioles in the cell cycle. I. Epithelial cells. *J. Cell Biol.* 93:938–949.
- Wong, C., and T. Stearns. 2003. Centrosome number is controlled by a centrosome-intrinsic block to reduplication. *Nat. Cell Biol.* 5:539–544.
- Zheng, Y., M.L. Wong, B. Alberts, and T. Mitchison. 1995. Nucleation of microtubule assembly by a gamma-tubulin-containing ring complex. *Nature*. 378:578–583.
- zur Hausen, H. 1996. Papillomavirus infections—a major cause of human cancers. *Biochim. Biophys. Acta*. 1288:F55–F78.